Journal of Theoretical Biology 492 (2020) 110190

Contents lists available at ScienceDirect

Journal of Theoretical Biology

journal homepage: www.elsevier.com/locate/jtb

Impact of influenza vaccine-modified infectivity on attack rate, case fatality ratio and mortality

Kyeongah Nah[a,b], Mahnaz Alavinejad[a,b], Ashrafur Rahman[a,c], Jane M Heffernan[b,d], Jianhong Wu[a,b,d,e,*]

[a] Laboratory for Industrial and Applied Mathematics, York University, Toronto, ON M3J 1P3, Canada
[b] Department of Mathematics and Statistics, York University, Toronto, ON M3J 1P3, Canada
[c] Department of Mathematics and Statistics, Oakland University, Rochester, MI 48309, USA
[d] Centre for Disease Modelling (CDM), York University, Toronto, ON M3J 1P3, Canada
[e] Fields-CQAM Laboratory of Mathematics for Public Health, York University, Toronto, ON M3J 1P3, Canada

ARTICLE INFO

Article history:
Received 6 June 2019
Revised 3 October 2019
Accepted 2 February 2020
Available online 6 February 2020

Keywords:
Attack rate
Attack ratio
Influenza virus
Vaccination impact
Mathematical modelling

ABSTRACT

Generally, vaccines are designed to provide protection against infection (susceptibility), disease (symptoms and transmissibility), and/or complications. In a recent study of influenza vaccination, it was observed that vaccinated yet infected individuals experienced increased transmission levels. In this paper, using a mathematical model of infection and transmission, we study the impact of vaccine-modified effects, including susceptibility and infectivity, on important epidemiological outcomes of an immunization program. The balance between vaccine-modified susceptibility, infectivity and recovery needed in preventing an influenza outbreak, or in mitigating the health outcomes of the outbreak is studied using the *SIRV*-type of disease transmission model. We also investigate the impact of influenza vaccination program on the infection risk of vaccinated and non-vaccinated individuals.

1. Introduction

Vaccination represents a major public health strategy for the prevention and control of many infectious diseases, including seasonal and pandemic influenza (Fiore et al., 2010; Osterholm et al., 2012). The successes of vaccination programs are often reported in terms of the measured reduction in the attack rate, defined as the proportion of a population that experiences influenza over the period of an influenza epidemic (Porta, 2014) (Note that since the time dimension in the attack rate is uncertain, the attack rate may be more appropriately called the attack ratio, or attack proportion). The reduced risk of infection of vaccinated individuals, calculated by the difference in attack rate among non-vaccinated and vaccinated individuals is also typically reported, as well as the case fatality ratio (the ratio of deaths occurring from an influenza infection to the total number of cases), the death rate of infected individuals (given the vaccination program), and the total number of infections over the epidemic (also known as the epidemic final size).

The total attack rate and the various other measures of vaccination program outcomes can depend on several different effects of vaccination in individuals. It is well known that vaccination can reduce susceptibility in vaccinated individuals (Jackson et al., 2010; Osterholm et al., 2012). This, in turn, can protect non-vaccinated contacts of these vaccinated individuals through herd immunity. A separate outcome of a vaccination program is a vaccine-modified disease experience (Belshe et al., 2000; Deiss et al., 2015; Talbot et al., 2005; VanWormer et al., 2014). Vaccinated yet infected individuals may experience milder symptoms than those experienced by infected individuals who are not vaccinated (Deiss et al., 2015; VanWormer et al., 2014). The infectious period may also be affected in that it may be reduced, giving a faster recovery time (Belshe et al., 2000; Talbot et al., 2005), and a reduction in pathogen shedding (Belshe et al., 2000). In a recent study by Yan et al. (Yan et al., 2018), it was observed that influenza viral shedding may be increased in vaccinated yet infected individuals. It has also been observed that symptom onset in vaccinated yet infected individuals may be delayed (Cao et al., 2015).

Here, we are interested in understanding how different outcomes of vaccination in individuals can affect public health measures of vaccination programs. Our focus is to examine the influence of vaccination on the infection risk of vaccinated and non-vaccinated individuals, and see how the results change when

* Corresponding author at: Department of Mathematics and Statistics, York University, 4700 Keele Street, Toronto, ON M3J 1P3, Canada.
E-mail addresses: wujh@mathstat.yorku.ca, wujh@yorku.ca (J. Wu).

https://doi.org/10.1016/j.jtbi.2020.110190
0022-5193/

Table 1
Parameters of the proposed *SIRV* model, with parameter ranges collected from published literature.

Symbol	Definition (Unit)	Range	Reference
R_0	Basic reproduction number	[1.47, 2.27]	Biggerstaff et al. (2014)
β	Baseline transmission rate (day^{-1} person^{-1})	Calculated	Eq. (4)
m_i	Vaccine-modified infectivity	[0, 6]	Yan et al. (2018)
γ	Recovery rate of non-vaccinated infecteds (day^{-1})	[0.14, 0.5]	CDC (2020b) Carrat et al. (2008)
m_r	Vaccine-modified recovery	$m_r < 1$	Talbot et al., (2005) Cao et al. (2016)
m_{SIO}	Relative risk of severe infection outcome in vaccinated infecteds to non-vaccinated infecteds	[0, 1]	
RR_{SIO}	Relative risk of severe infection outcome in vaccinated individuals to non-vaccinated individuals	Calculated	Eq. (16)
δ	Disease-induced mortality (day^{-1})	$[0.2, 2] \times 10^{-3}$	Eq. (5),
m_d	Vaccine-modified mortality	[0, 1]	Fireman et al. (2009)
m_s	Vaccine-modified susceptibility	[0, 0.6]	Basta et al. (2008)
ρ	Vaccine coverage	[0, 1]	
N_0	Population size at $t = 0$ (person)	1000	Assumed

vaccine coverage and vaccine-modified effects are varied. For this purpose, we develop a mathematical model that incorporates variations in susceptibility, pathogen shedding and infection period in all vaccinated individuals. We formulate our model and interpret the analyses for influenza infection so as to directly consider the outcomes observed in Yan et al. (2018), however, our approach is generic and can be applied to other infections with corresponding vaccines.

2. Model

We extend the basic Susceptible-Infected-Recovered-Vaccinated (*SIRV*) model to include an vaccinated yet infected class I_V, to study the effects of vaccine-modified susceptibility and transmissibilty. We assume that vaccination is implemented prior to an influenza season with coverage ρ, giving an initial number of non-vaccinated and vaccinated susceptibles $S(0) = (1-\rho)N_0$ and $V(0) = \rho N_0$, respectively. Here, we let β denote the transmission rate of non-vaccinated individuals, and we let m_i denote the modification factor of the transmission rate for vaccinated individuals. That is, βm_i is the transmission rate of a vaccinated individual. We also use m_s to denote the reduction in susceptibility of vaccinated susceptible individuals. Additionally, the recovery rates in non-vaccinated and vaccinated infected individuals are denoted by γ and $m_r\gamma$, respectively, where m_r represents the vaccine-modified recovery. Finally, disease-induced mortality is represented by δ and $m_d\delta$ for non-vaccinated and vaccinated individuals, respectively, with $0 < m_d < 1$ representing a reduction in mortality of vaccinated individuals (Fireman et al., 2009). The model is written as

$$\begin{cases} \dfrac{dS}{dt} = -\beta S(I + m_i I_V), \\ \dfrac{dV}{dt} = -\beta m_s V(I + m_i I_V), \\ \dfrac{dI}{dt} = \beta S(I + m_i I_V) - \gamma I - \delta I, \\ \dfrac{dI_V}{dt} = \beta m_s V(I + m_i I_V) - m_r\gamma I_V - m_d\delta I_V \\ \dfrac{dR}{dt} = \gamma I + m_r\gamma I_V, \end{cases}$$

where $S(0) = (1-\rho)N_0$, $V(0) = \rho N_0$, N_0 is the initial total population. In the following, we refer to the model as the *SIRV* model. Model parameters are listed in Table 1.

2.1. Final size equation

We derive the final size equations of the *SIRV* model, giving the number of non-vaccinated and susceptible (S), vaccinated and susceptible (V), and recovered (R) individuals at the end of an outbreak. In the following formulations, we let S_∞ be the limit of $S(t)$ as $t \to \infty$, marking the end of the outbreak. Similarly, we define V_∞ and R_∞. Dividing the first and second equations of the *SIRV* model by S and V, respectively, and integrating, we obtain:

$$\begin{cases} \ln \frac{S(0)}{S_\infty} = \beta(\hat{I} + m_i\hat{I}_V), \\ \ln \frac{V(0)}{V_\infty} = \beta m_s(\hat{I} + m_i\hat{I}_V), \end{cases}$$

where

$$\hat{I} = \frac{S(0) - S_\infty + I(0)}{\gamma + \delta},$$
$$\hat{I}_V = \frac{V(0) - V_\infty + I_V(0)}{m_r\gamma + m_d\delta}$$

are determined by adding the first and third, and the second and fourth equations of the *SIRV* model, and integrating. Substituting these into the equations for $\ln \frac{S(0)}{S_\infty}$ and $\ln \frac{V(0)}{V_\infty}$ yields

$$\begin{aligned} \ln \frac{S(0)}{S_\infty} &= \frac{\beta}{\gamma+\delta}(S(0) - S_\infty) + \frac{m_i\beta}{m_r\gamma + m_d\delta}V(0)\left(1 - \left(\frac{S_\infty}{S(0)}\right)^{m_s}\right) \\ &\quad + \frac{\beta}{\gamma+\delta}I(0) + \frac{m_i\beta}{m_r\gamma + m_d\delta}I_V(0), \\ V_\infty &= V(0)\left(\frac{S_\infty}{S(0)}\right)^{m_s}. \end{aligned} \tag{1}$$

To determine R_∞ we integrate the fifth equation of the *SIRV* model to obtain $R_\infty = \gamma\hat{I} + m_r\gamma\hat{I}_V$, and

$$R_\infty = \gamma\frac{S(0) - S_\infty + I(0)}{\gamma + \delta} + m_r\gamma\frac{V(0) - V_\infty + I_V(0)}{m_r\gamma + m_d\delta}.$$

Note that a more general form of the final size relation (1) is introduced in Arino et al. (2007).

2.2. Measures used to assess the impact of vaccination

The following measures are used to assess the impact of vaccination on the total population and all subpopulations.

2.2.1. Reproduction numbers, R_0 and R_v

At the disease free equilibrium $((1-\rho)N_0, \rho N_0, 0, 0, 0)$ we have the linearization

$$J = \begin{pmatrix} 0 & 0 & -\beta(1-\rho)N_0 & -\beta m_i(1-\rho)N_0 & 0 \\ 0 & 0 & -\beta m_s\rho N_0 & -\beta m_s m_i\rho N_0 & 0 \\ 0 & 0 & \beta(1-\rho)N_0 - (\gamma+\delta) & \beta m_i(1-\rho)N_0 & 0 \\ 0 & 0 & \beta m_s\rho N_0 & \beta m_s m_i\rho N_0 - (m_r\gamma + m_d\delta) & 0 \\ 0 & 0 & \gamma & m_r\gamma & 0 \end{pmatrix}.$$

Using a standard application of the next generation matrix approach (Van den Driessche and Watmough, 2008), we obtain that the control reproduction number R_v is

$$R_v = \frac{\beta}{\gamma+\delta}(1-\rho)N_0 + \frac{m_i m_s \beta}{m_r\gamma + m_d\delta}\rho N_0 . \quad (2)$$

When there is no control effort ($\rho = 0$), R_v is equal to the basic reproduction number (R_0):

$$R_0 = \frac{\beta}{\gamma+\delta}N_0.$$

*2.2.2. Final size (*F*)*

The final size of an epidemic is given by the cumulative number of all individuals who have experienced influenza infection (either recovered or dead). This can be written as $F = F_v + F_n$, where $F_v = V(0) - V_\infty$ and $F_n = S(0) - S_\infty$ denote the final size of the vaccinated and non-vaccinated populations, respectively.

*2.2.3. Attack rate (*A*)*

The attack rate, the cumulative incidence over a period of the influenza season, is estimated by dividing the epidemic final size F by the total population at the beginning of the epidemic: $A = (N_0 - S_\infty - V_\infty)/N_0$. The attack rate can be re-written as $A = \rho A_v + (1-\rho)A_n$, where ρ and $1-\rho$ are the proportions of vaccinated and non-vaccinated individuals, respectively, and $A_v = \frac{\rho N_0 - V_\infty}{\rho N_0}$ and $A_n = \frac{(1-\rho)N_0 - S_\infty}{(1-\rho)N_0}$ are the attack rates on these populations.

*2.2.4. Case fatality ratio (*CFR*)*

The case fatality ratio, the proportion of disease-induced death among all infected individuals, is estimated by the ratio of the number of influenza-induced deaths and the total number of individuals who experienced influenza infection over the course of the epidemic: $CFR = (N_0 - S_\infty - V_\infty - R_\infty)/(N_0 - S_\infty - V_\infty)$.

2.2.5. Death rate (per 100,000 population)

The death rate (per 100,000) is given by

$$\text{Death rate} = \frac{N_0 - S_\infty - V_\infty - R_\infty}{N_0} \times 10^5. \quad (3)$$

2.3. Parameter values

Parameter values are determined from the published literature (observational and clinical studies). Parameter values are listed in Table 1. Details are given below:

2.3.1. Disease transmission rate (β)

We determine the transmission rate from parameters δ, γ, and the basic reproduction number R_0 of the 1918 influenza pandemic, using the relation

$$\beta = R_0\frac{\delta+\gamma}{N_0}. \quad (4)$$

Note that the basic reproduction number (R_0) is equal to the control reproduction number without control effort ($\rho = 0$) (which was the case for the 1918 pandemic). A systematic review on the estimates of the reproduction number of 1918 pandemic reported the median of reproduction number as 1.80 with interquartile range [1.47, 2.27] (Biggerstaff et al., 2014).

2.3.2. Vaccine-modified infectivity (m_i)

The value of m_i lies in the interval [0,1) if it is assumed that vaccinated but infected individuals are less infectious than non-vaccinated individuals. The study (Yan et al., 2018) observed that vaccinated individuals could pose a higher level of infectivity. It was observed that fine-aerosol shedding among cases with vaccination was 6 times higher than that measured in infected individuals who were not vaccinated. It was also observed that vaccination had no effect on course-aerosol shedding. In a recent study it was estimated that exposure to 10 times the size of an infectious dose could result in a 0.28 increase in the log-odds of infection (Earn et al., 2014). While this does not translate to a linear relationship between increase in viral shedding and infectivity, for simplicity, we continue herewithin with the assumption that a 6-fold increase in viral shedding may increase infectivity by the same magnitude (i.e., m_i takes on values within the range [0, 6]).

2.3.3. Recovery rates (γ and $m_r\gamma$)

It is known that infected people are most contagious during the first 3–4 days after symptom onset and contagious for approximately 5 days after symptom onset (Carrat et al., 2008; CDC, 2020b). Taking into account the average incubation period of 2 days (CDC, 2020a), we consider the recovery rate γ to lie in the interval [0.14, 0.5]. It is assumed that vaccination can modify the period of infection. Here, we assume that the recovery rate can be increased ($m_r > 1$) so that the infectious period is shortened, representing a shorter course of infection (Talbot et al., 2005). However, we also assume that vaccinated individuals can experience a milder infection with a lengthened infectious period ($m_r < 1$). This assumption is supported by two arguments. Previous modelling studies have shown that memory T-cells are needed in order for a shortened infectious period to be experienced (Cao et al., 2016; Yan et al., 2017). Therefore, if vaccination induces only memory B-cells and antibodies, the infectious period would not be shortened. Additionally, Yan et al. (2018) acquired shedding data from vaccinated and non-vaccinated infected individuals 1–2 days after symptom onset. Given that vaccinated individuals may show symptoms at a later time point in infection compared to non-vaccinated infected individuals (i.e., the activated immune system in vaccinated individuals can delay the onset of symptoms and reduce symptom severity (Cao et al., 2015; Deiss et al., 2015; VanWormer et al., 2014)), it may be assumed that the infection period in vaccinated individuals is lengthened.

2.3.4. Vaccine-modified susceptibility (m_s)

A study by Basta et al. (2008) estimated the absolute vaccine efficacy for susceptibility using the data from experimental influenza challenge studies. Both live influenza vaccine and inactivated vaccine provided 40% protection against laboratory-confirmed infection. Therefore, we set the maximum estimate of vaccine-modified susceptibility m_s to be 0.6.

2.3.5. Disease-induced mortality (δ)

The disease-induced mortality ratio δ is related to the case-fatality ratio (CFR), by

$$CFR = \frac{m_d\delta}{m_r\gamma + m_d\delta}\frac{\rho A_v}{A} + \frac{\delta}{\gamma+\delta}\frac{(1-\rho)A_n}{A}, \quad (5)$$

where m_d is the vaccine-modified mortality, m_r is the vaccine-modified recovery, γ is the recovery rate, ρ is the vaccine coverage, A, A_v, A_n are the attack rates of total population, vaccinated sub-population and non-vaccinated sub-population, respectively. According to a systemic review (Wong et al., 2013), the case fatality risk of pandemic influenza can range from 1 to $> 10,000$ deaths per 100,000 infections. Therefore, we consider the range of the parameter δ so that the resulting CFR lies between 0.001% and 10%.

2.3.6. Vaccine-modified mortality (m_d)

Fireman et al. (2009) estimated vaccine effectiveness against all-cause mortality during an influenza season to be 4.6%. We

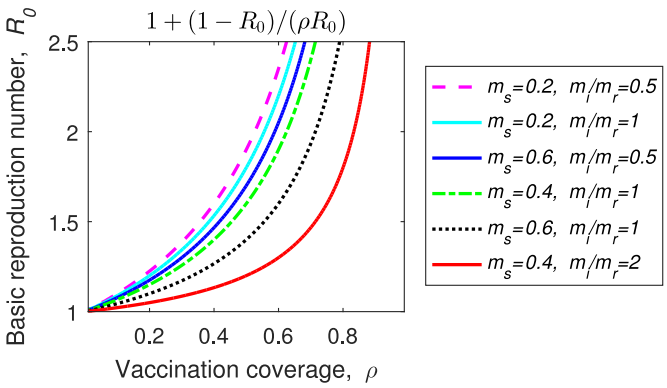

Fig. 1. Basic reproduction number (R_0) and vaccine coverage (ρ) characterizing vaccine-modified effects at the epidemic threshold $R_v = 1$. The figure gives a contour plot for the left side of the Eq. (6), given fixed values of the right side of this equation.

assume that vaccination can reduce the risk of death upon infection, and limit m_d such that $0 \le m_d \le 1$.

3. Results

We assess the effectiveness of vaccination by observing the influence of vaccine coverage on the control reproduction number, final size, attack rate, CFR and the death rate (Eqs. (2) and (3)). We study the influence of vaccination on the infection risk of vaccinated and non-vaccinated individuals, and see how the results change when the vaccine coverage (ρ), vaccine-modified susceptibility (m_s), vaccine-modified infectivity (m_i), and vaccine-modified recovery (m_r) are varied. The results are presented in the following subsections.

3.1. The relationship between vaccine-modified effects and the epidemic threshold

When a vaccination program is in place a control reproduction number $R_v = 1$ provides the threshold that determines when an influenza epidemic will occur (i.e, when $R_v < 1$ there is no epidemic, when $R_v > 1$, the infection will spread). Ignoring disease-induced mortality (assuming that $\delta \ll \gamma$, where δ is the disease-induced mortality and γ is the recovery rate), Eq. (2) is reduced to

$$R_v = (1-\rho)R_0 + \frac{m_i m_s}{m_r}\rho R_0 .$$

Rearranging this, we have that $R_v < 1$ if and only if

$$1 + \frac{1-R_0}{\rho R_0} > m_s \frac{m_i}{m_r}. \tag{6}$$

Thus, we quantify the condition for an epidemic that involves a direct relationship between the epidemiological characteristics of an influenza epidemic (a basic reproduction number R_0 and the vaccine coverage ρ representing the control effort), and the in-host (individual) level parameters of vaccination m_s (vaccine-modified susceptibility), m_i (vaccine-modified infectivity) and m_r (vaccine-modified recovery). Note that, henceforth, we interpret m_i/m_r as the vaccine-modified viral shedding. A contour plot of the left hand side of Eq. (6) is shown in Fig. 1 for different values of m_s and m_i/m_r. Here, we observe that to achieve $R_v < 1$, $m_s m_i/m_r$ must increase as ρ increases, and can decrease when R_0 decreases. We also find that a higher vaccination coverage (ρ) and a lower R_0 allows less strict vaccine-modified susceptibility and infectiousness. Therefore, allowing a higher vaccine-modified susceptibility or infectivity (m_s, m_i), or a lower vaccine-modified recovery rate (m_r) can still maintain $R_v < 1$.

Differentiating both sides of Eq. (2) with respect to ρ, the vaccination coverage, we find

$$\frac{\partial R_v}{\partial \rho} = -\frac{\beta}{\gamma+\delta}N_0 + \frac{m_i m_s \beta}{m_r\gamma + m_d\delta}N_0. \tag{7}$$

Therefore, the control reproduction number R_v is an increasing (decreasing) function of the vaccination coverage ρ when m_s is greater (less) than the threshold m_s^*, where

$$m_s^* = \frac{1}{m_i}\frac{m_r\gamma + m_d\delta}{\gamma+\delta}, \quad \text{or} \quad m_s^* = \frac{m_r}{m_i} \tag{8}$$

when disease-induced death is negligible ($\delta = 0$). Therefore, a balance between m_s, m_i and m_r is needed to achieve $R_v < 1$. This can also be observed in Fig. 1.

3.2. The impact of vaccination on the attack rates

In this section, we study the dependence of the attack rate (A) on the vaccination coverage (ρ) and the vaccine-modified effects on susceptibility, infectivity and recovery (m_s, m_i and m_r).

When disease-induced mortality is negligible ($\delta = 0$), the final size relation Eq. (1) is reduced to

$$\begin{aligned} -\ln(1-A_n) &= (1-\rho)R_0A_n + \frac{m_i}{m_r}\rho R_0 A_v, \\ A_v &= 1-(1-A_n)^{m_s}, \end{aligned} \tag{9}$$

where $A_v = 1 - \frac{V_\infty}{\rho N_0}$ and $A_n = 1 - \frac{S_\infty}{(1-\rho)N_0}$ are the attack rates among vaccinated and non-vaccinated individuals, respectively. Observe from Eq. (9) that changing m_i by a certain percent is equivalent to a change in $1/m_r$ by the same fraction. Therefore, in the following, we will limit our observations on the dependence of the attack rate on the vaccine-modified viral shedding (m_i/m_r) and vaccine-modified susceptibility (m_s) only.

3.2.1. Attack rate in the total population

Figs. 2 and 3 plot the attack rate against the vaccination coverage ρ when the vaccine-modified viral shedding m_i/m_r and vaccine-modified susceptibility m_s are varied. Results show that, when $m_i/m_r < 1$, the attack rate (A) decreases as vaccine coverage (ρ) increases. We also observe, however, that increased vaccination coverage ρ does not guarantee a reduced attack rate when $m_i/m_r > 1$ unless the vaccine modified susceptibility m_s is sufficiently small (see Fig. 2b for an example).

The solid blue curves in Figs. 2a and b, and 3a seperate the parameter space into two regions. Here, we observe that the attack rate increases (decreases) as vaccination coverage ρ increases above (below) these curves. We can identify the parameter regions discussed here by observing the numerical value of $\partial A/\partial\rho$ (blue curves in left panels of Figs. 2 and 3). Differentiating both sides of the equation

$$A = \rho A_v + (1-\rho)A_n, \tag{10}$$

we obtain

$$\frac{\partial A}{\partial \rho} = A_v + \rho\frac{\partial A_v}{\partial\rho} - A_n + (1-\rho)\frac{\partial A_n}{\partial\rho}. \tag{11}$$

When disease induced mortality is negligible ($\delta = 0$), the final size relation is reduced to

$$\begin{aligned} -\ln(1-A_n) &= (1-\rho)R_0A_n + \frac{m_i}{m_r}\rho R_0 A_v; \\ A_v &= 1-(1-A_n)^{m_s}. \end{aligned} \tag{12}$$

Differentiating both sides of the equations with respect to ρ, we obtain

$$\frac{1}{1-A_n}\frac{\partial A_n}{\partial\rho} = -R_0A_n + (1-\rho)R_0\frac{\partial A_n}{\partial\rho} + \frac{m_i}{m_r}R_0A_v + \frac{m_i}{m_r}\rho R_0\frac{\partial A_v}{\partial\rho} \tag{13}$$

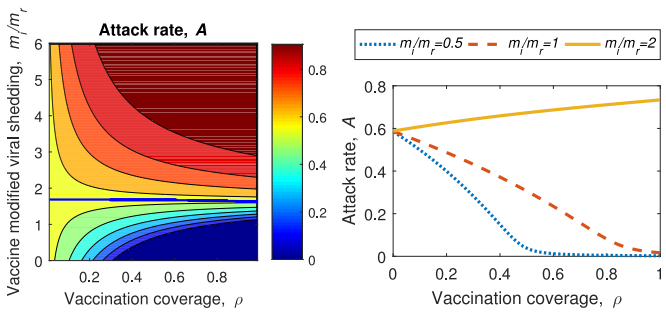

(a) With a fixed vaccine-modified susceptibility, $m_s = 0.6$.

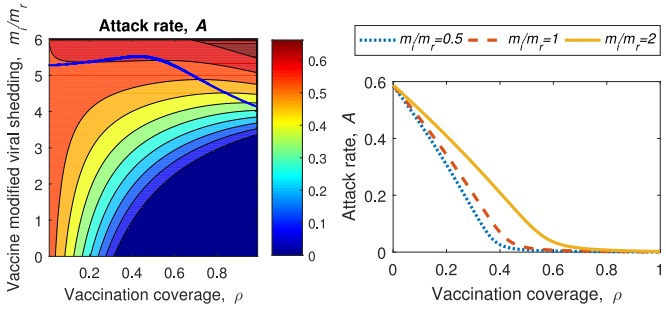

(b) With a fixed vaccine-modified susceptibility, $m_s = 0.2$.

Fig. 2. Dependence of attack rate (A) on the vaccine coverage (ρ) and the vaccine-modified viral shedding (m_i/m_r). In the simulation we set $R_0 = 1.5$, $\gamma = 0.33$, and $m_s = 0.6$ (top row) or $m_s = 0.2$ (bottom row). We ignore disease-induced death ($\delta = 0$). Left column: Heat map of the attack rate depending on the vaccine coverage and vaccine-modified viral shedding. The blue curve represents $\partial A/\partial\rho = 0$. Right column: Relation between vaccine coverage (ρ) and attack rate (A) with various vaccine-modified viral shedding, $m_i/m_r = 0.5$ (dotted blue), $m_i/m_r = 1$ (red dashed line) and $m_i/m_r = 2$ (yellow line). (For interpretation of the references to colour in this figure legend, the reader is referred to the web version of this article.)

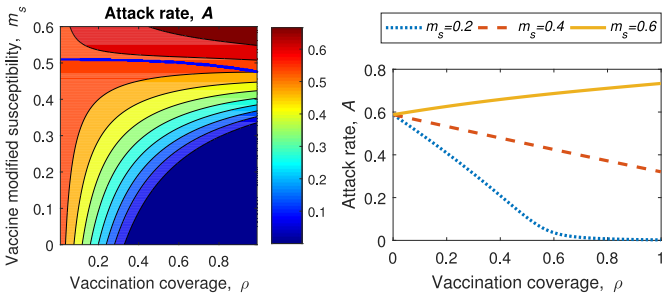

(a) With a fixed vaccine-modified viral shedding, $m_i/m_r = 2$.

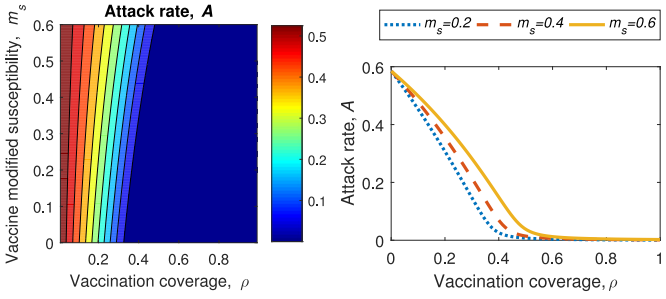

(b) With a fixed vaccine-modified viral shedding, $m_i/m_r = 0.5$.

Fig. 3. Dependence of attack rate (A) on the vaccine coverage (ρ) and the vaccine-modified susceptibility (m_s). In the simulation we set $R_0 = 1.5$, $\gamma = 0.33$, and $m_i/m_r = 2$ (top row) or $m_i/m_r = 0.5$ (bottom row). Here, $m_s^* = 1/2$ (top row) and $m_s^* = 2$ (bottom row). We ignore disease-induced death ($\delta = 0$). Left column: Heat map of the attack rate depending on the vaccine coverage (ρ) and vaccine-modified susceptibility (m_s). The blue curve represents $\partial A/\partial\rho = 0$. Right column: Relation between vaccine coverage (ρ) and the attack rate (A) with various vaccine-modified susceptibilities, $m_s = 0.2$ (dotted blue), $m_s = 0.4$ (red dashed line) and $m_s = 0.6$ (yellow line). (For interpretation of the references to colour in this figure legend, the reader is referred to the web version of this article.)

where

$$\frac{\partial A_v}{\partial \rho} = m_s(1-A_n)^{m_s-1}\frac{\partial A_n}{\partial \rho}. \tag{14}$$

Using Eqs. (10), (13) and (14), we have

$$\frac{1}{1-A_n}\frac{\partial A_n}{\partial \rho} = -R_0A_n + (1-\rho)R_0\frac{\partial A_n}{\partial \rho} + \frac{m_i}{m_r}R_0(1-(1-A_n)^{m_s}) + \frac{m_i}{m_r}\rho R_0 m_s(1-A_n)^{m_s-1}\frac{\partial A_n}{\partial \rho}$$

which can be re-written as

$$\frac{\partial A_n}{\partial \rho} = \frac{-R_0A_n + \frac{m_i}{m_r}R_0(1-(1-A_n)^{m_s})}{(1-A_n)^{-1} - (1-\rho)R_0 - \rho m_s\frac{m_i}{m_r}R_0(1-A_n)^{m_s-1}}. \tag{15}$$

Therefore, the numerical value of $\frac{\partial A}{\partial \rho}$ can be determined using Eqs. (10), (11), (14), (15). Note that the solid blue curves in Figs. 2a and b, and 3a correspond to the value $\frac{\partial A}{\partial \rho} = 0$. For reference, Fig. 4 shows $\frac{\partial A}{\partial \rho}$ and $sgn(\frac{\partial A}{\partial \rho})$ on the $\rho - m_s$ parameter plane.

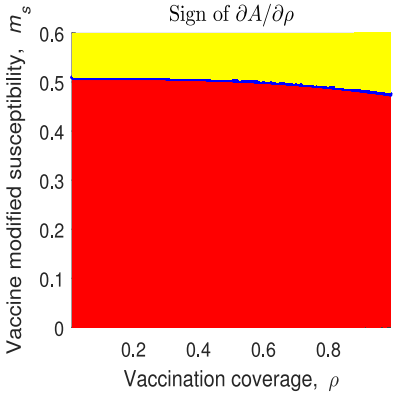

Fig. 4. $\frac{\partial A}{\partial \rho}$ (left panel) and $sgn(\frac{\partial A}{\partial \rho})$ (right panel) in the $\rho - m_s$ parameter plane, corresponding to Fig. 3 (top panel) in the paper. The yellow [red] region in the right panel corresponds to $\frac{\partial A}{\partial \rho} > 0$ $\left[\frac{\partial A}{\partial \rho} < 0\right]$. Here, $R_0 = 1.5$, $\gamma = 0.33$, $\delta = 0$, $N_0 = 1000$ and $m_i/m_r = 2$. (For interpretation of the references to colour in this figure legend, the reader is referred to the web version of this article.)

3.2.2. Attack rate in vaccinated and non-vaccinated populations

In the last section, we showed that the increased vaccine coverage does not guarantee a reduced attack rate. Here we show that, as long as the vaccine lowers the susceptibility of a vaccinated indivdiual, this individual will have a lower chance of infection compared to non-vaccinated individuals. Specifically, when the vaccine-modified susceptibility is less than one ($m_s < 1$), the attack rate of vaccinated individuals is less than the attack rate of non-vaccinated individuals ($A_v < A_n$) regardless of vaccine coverage or other vaccine-modified effects. This can be shown from the second equation of (12), $A_v = 1-(1-A_n)^{m_s}$. By subtracting A_n from both sides of the equation, we have $A_v - A_n = (1-A_n)(1-(1-A_n)^{m_s-1})$, which is negative when $m_s < 1$.

The left panel in Fig. 5 presents the attack rates in the total population, vaccinated and non-vaccinated populations. In this figure, vaccine-modified susceptibility is set to be less than one ($m_s < 1$) which results the attack rate of the vaccinated population to be less than that of the non-vaccinated population ($A_v < A_n$). In the simulation, the vaccine-modified susceptibility is set to be 0.4 (m_s=0.4). In this case, as observed in Fig. 4, we

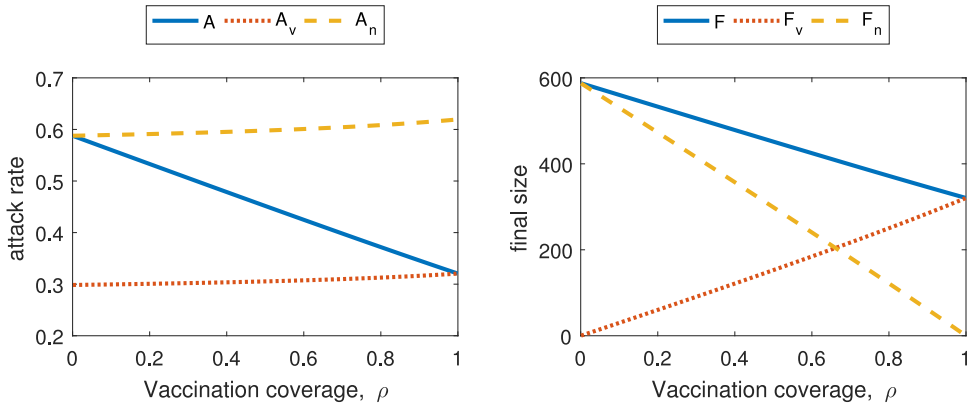

Fig. 5. Attack rates and epidemic final sizes. The attack rates A, A_v, and A_n (left panel) and epidemic final sizes F, F_v, and F_n (right panel) are shown. Right (left) panel represents the total number of infecteds (attack rate) for the general population (solid curve), and the vaccinated (dotted curve) and non-vaccinated (dashed curve) individuals. The parameter values are set as $m_s = 0.4$, $m_i/m_r = 2$, $R_0 = 1.5$, $\gamma = 0.33$, $\delta = 0$. Here, $m_s < m_s^* = 0.5$.

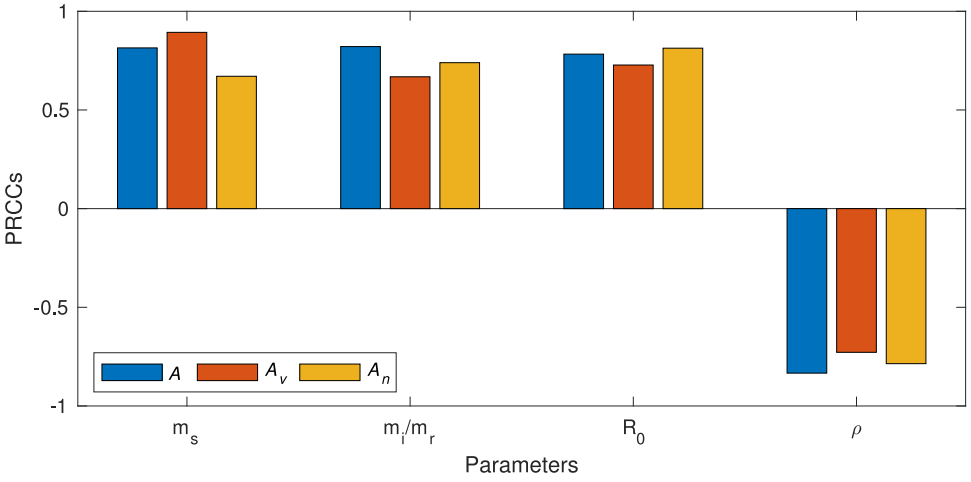

Fig. 6. Sensitivity results (PRCCs) Among 5000 sets of sample parameters drawn by a Latin Hypercube Sampling from a set of uniform distributions, 4666 sets which satisfy $R_v > 1$ were chosen. For the sensitivity of A, A_v and A_n, we have further selected 2298, 1338, 1338 sample parameters which satisfy $\frac{\partial A}{\partial \rho} < 0$, $\frac{\partial A_v}{\partial \rho} < 0$ and $\frac{\partial A_n}{\partial \rho} < 0$, respectively. Parameter ranges used in the simulations are $m_s \in [0.1, 0.6]$, $m_i/m_r \in [0.5, 6]$, $R_0 \in [1.47, 2.27]$ and $\rho \in [0.1, 0.9]$. Here, $\gamma = 0.33$ and $N_0 = 1000$ are assumed.

have $\frac{\partial A}{\partial \rho} < 0$ and the attack rate in the total population (blue line in Fig. 5) decreases with increasing vaccine coverage. On the other hand, in this particular case, attack rates for vaccinated individuals and non-vaccines are increasing with respect to the vaccine coverage.

Fig. 6 shows the partial rank correlation coefficients of parameters m_s (vaccine-modified susceptibility), m_i/m_r (vaccine-modified viral shedding), R_0 (basic reproduction number) and ρ (vaccine coverage) on the attack rates A, A_v and A_n. Parameters are assumed to follow a uniform distribution within the ranges depicted in the caption. Parameter sets ($n = 5000$) were chosen using Latin Hypercube sampling. Among those parameter sets ($n = 5000$), we selected the parameter sets which induce an influenza outbreak ($R_v > 1$, $n = 4668$) and studied their correlation with the attack rates. For the sensitivity of attack rate in the total population (A), vaccinated population (A_v) and non-vaccinated population (A_n), we have further selected parameters ($n = 2281$, $n = 1332$, $n = 1332$) which satisfy $\frac{\partial A}{\partial \rho} < 0$, $\frac{\partial A_v}{\partial \rho} < 0$ and $\frac{\partial A_n}{\partial \rho} < 0$, respectively. These parameter sets are chosen for the monotonic relationship between vaccine coverage (ρ) and attack rates (A, A_v and A_n), ensuring effectiveness of the vaccination program in reducing attack rates of each population groups (total, vaccinated and non-vaccinated populations). Here, we observe significant (PRCC magnitude > 0.5) positive correlations between A, A_v and A_n with m_s, m_i/m_r and R_0.

3.3. The impact of vaccination on other public health outcomes

We now consider the impact of vaccination on of the final size (F), CFR and death rate. Hereafter, we focus on vaccines with strong enough protection effects ($m_s < m_s^*$) which yields $\frac{\partial R_v}{\partial \rho} < 0$ (Eq. (7)), considering only the effective vaccination scenario.

Fig. 5 shows the attack rates and final sizes for the general population (A, F), and the vaccinated (A_v, F_v) and non-vaccinated (A_n, F_n) sub-populations. When vaccinated individuals are less susceptible than non-vaccinated individuals ($m_s < 1$), the infection risk of vaccinated individuals (A_v) is always less than the risk of non-vaccinated individuals (A_n); however, the final size of the vaccinated individuals (F_v) may exceed the final size of the non-vaccinated individuals (F_n) as seen in the right panel of Fig. 5.

Fig. 7 shows the dependence of the CFR (case fatality ratio) and the death rate on the vaccine coverage and the vaccine-modified effects on susceptibility, infectivity and recovery. As we see from Fig. 7b and c, vaccination will reduce the number of deaths and CFR when the vaccine-modified infectivity (m_i) is small enough and vaccine-modified recovery (m_r) is high enough. Higher vaccine protection effect corresponding to lower vaccine susceptibility (m_s) will result in a lower number of influenza deaths but higher CFR, see Fig. 7a. This suggests that vaccines with a strong protection effect against influenza infection ($m_s << 1$) will help reduce the number of influenza deaths by lowering the number of influenza

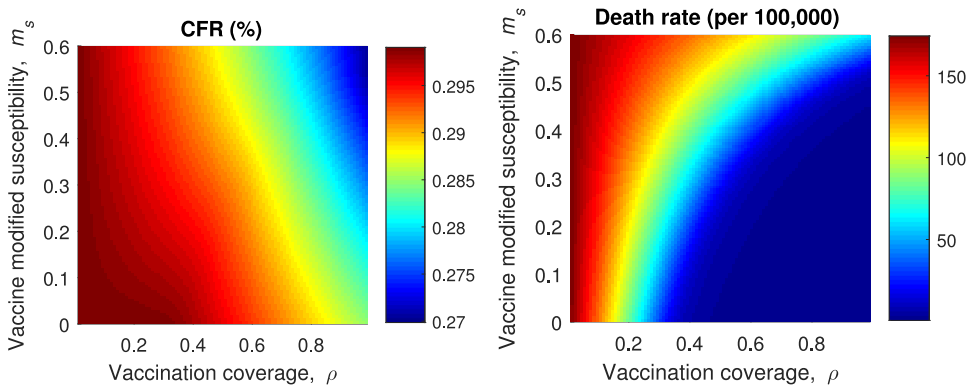

(a) With varying vaccine-modified susceptibility

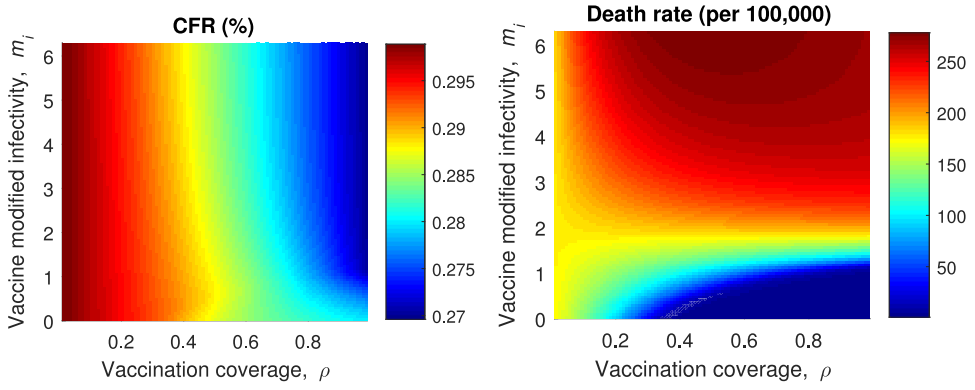

(b) With varying vaccine-modified infectivity

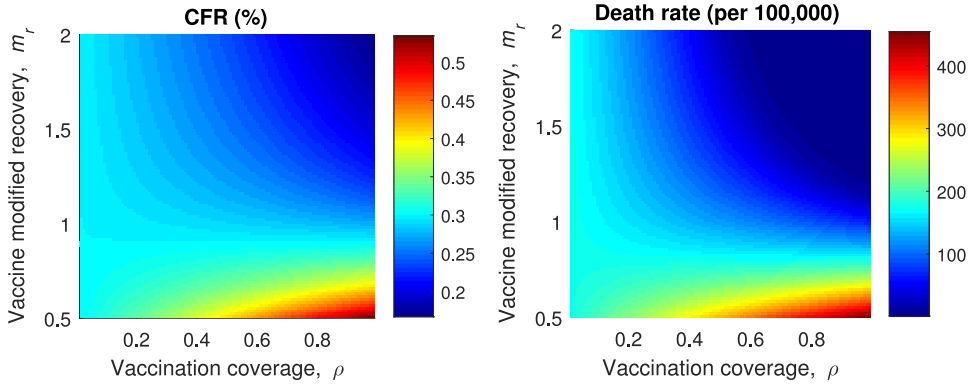

(c) With varying vaccine-modified recovery

Fig. 7. Dependence of CFR and probability of death on the vaccine coverage and the vaccine-modified effects. In the simulation, we set the basic reproduction number as 1.5 ($R_0 = 1.5$) and the contagious period of non-vaccinated infecteds as 3 days ($\gamma = 0.33$). The disease-induced mortality is set to be 10^{-3} ($\delta = 10^{-3}$) with vaccine-modified mortality $m_d = 0.9$. In Fig. 7a and b, we assume that the vaccine does not modify the contagious period ($m_r = 1$). In Fig. 7a and c, we assume that the vaccine increase the infectivity of the vaccinated yet infected individuals by 1.25 times ($m_i = 1.25$). In Fig. 7b and c, we assume that the vaccine reduce the susceptibility of vaccinated individuals by 40% ($m_s = 0.6$).

infecteds, but, this may increase the CFR. Vaccination with high vaccine-modified recovery with faster recovery time will help reduce the CFR.

Figs. 8 and 9 show the sensitivity of the death rate and CFR with respect to the parameters on the vaccine-modified effects. We observe that the vaccine-modified susceptibility m_s, vaccine-modified infectivity m_i, basic reproduction number R_0 and the disease-induced mortality δ are positively correlated with the death rate. The vaccine-modified recovery m_r is negatively correlated with both the death rate and the CFR.

3.4. Weak vs strong vaccine outcomes

We now consider the effects of two vaccines that confer weak (Type 1) or strong (Type 2) protection against infection and transmission (see Table 2). Here, we assume that the weak vaccine confers only a mild reduction in susceptibility and severity, and that the strong vaccine confers a larger reduction. We, however, also assume that the stronger vaccine includes an increase in viral shedding (m_i/m_r).

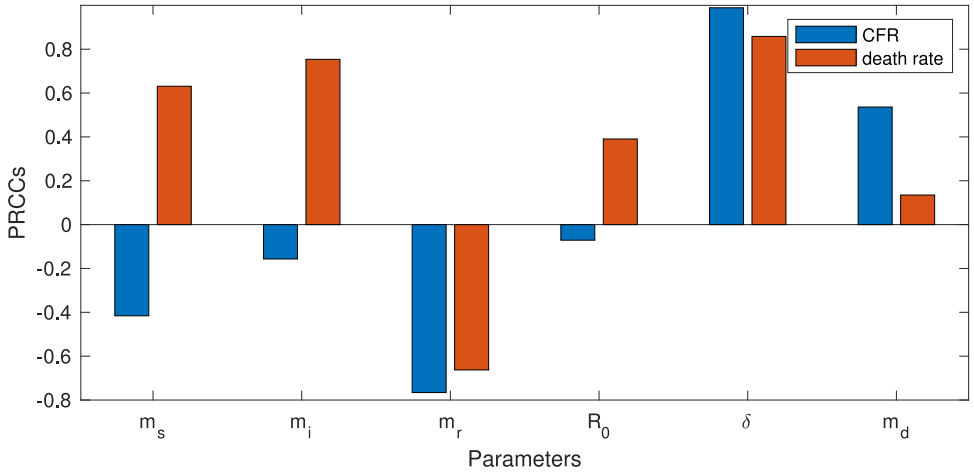

Fig. 8. PRCCs results of the parameters with respect to CFR and death rate. Among 5000 sets of sample parameters drawn by a Latin Hypercube Sampling from a set of uniform distributions, 4646 sets which satisfies $R_v > 1$ were chosen, excluding the parameters that do not induce an influenza outbreak. The range of parameters are $m_s \in [0.1, 0.6]$, $m_i/m_r \in [0.5, 6]$, [$m_i \in [0.1, 6]$, $m_r \in [0.5, 2]$] $R_0 \in [1.47, 2.27]$, $\delta \in [2 \times 10^{-4}, 2 \times 10^{-3}]$ and $m_d \in [0.5, 0.99]$. Initial population, recovery rate and the vaccine coverage are set to be 1000 ($N_0 = 1000$), 0.33 ($\gamma = 0.33$), 50% ($\rho = 0.5$), respectively.

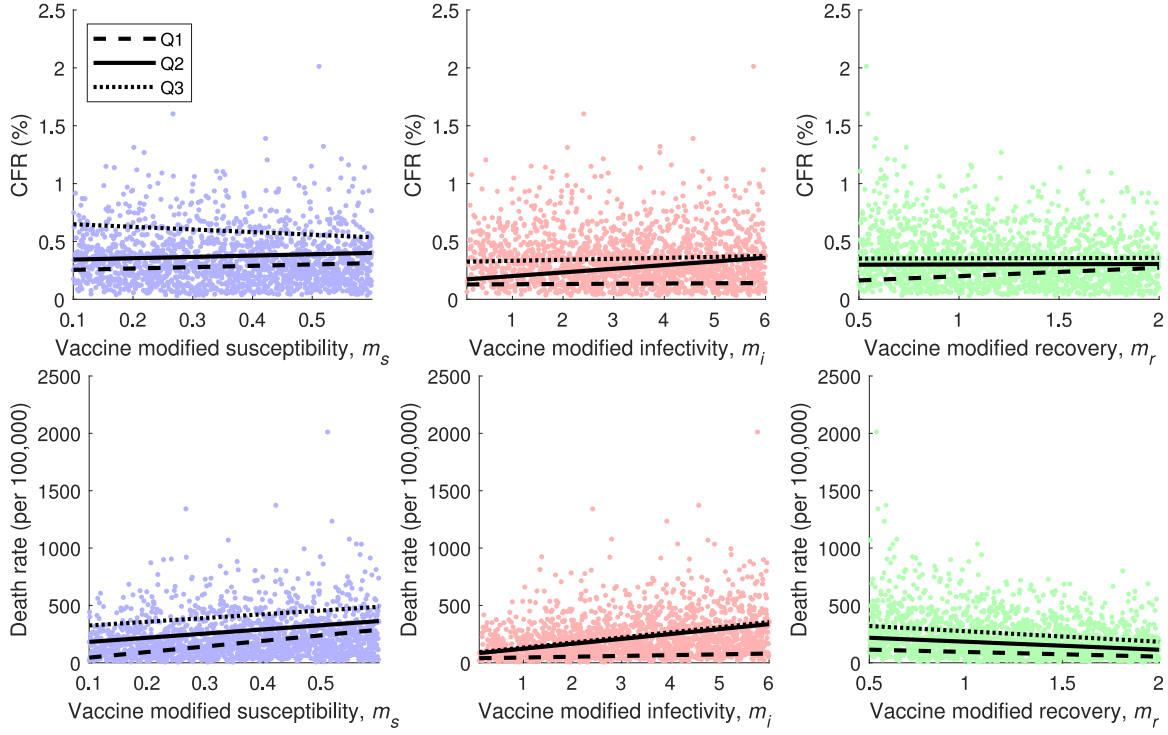

Fig. 9. Sensitivity of CFR and death rate with respect to vaccine-modified susceptibility (m_s), vaccine-modified infectivity (m_i) and vaccine-modified recovery (m_r). Panels in upper and lower sides are the scatter plots of the parameters and CFR, death rates per 100,000 population, respectively. Among 2000 set of sample parameters drawn by a Latin Hypercube Sampling from a set of uniform distributions, 1782 set which satisfies $R_v > 1$ were chosen. The lines show the quantile linear regression (Cade and Noon, 2003) of CFR and death rate as a function of each vaccine-modified effects. The dashed, solid and dotted lines represent the slope estimation for the 0.25, 0.5 and 0.75 quantiles. The range of parameters are $m_s \in [0.1, 0.6]$, $m_i \in [0.1, 6]$, $m_r \in [0.5, 2]$, $R_0 \in [1.47, 2.27]$, $\gamma \in [0.14, 0.5]$, $\rho \in [0.1, 0.9]$, $\delta \in [2 \times 10^{-4}, 2 \times 10^{-3}]$ and $m_d \in [0.5, 0.99]$. Initial population is set to be 1000 ($N_0 = 1000$).

Table 2
Types of hypothetical vaccines.

Vaccines	susceptibility (m_s)	severity (m_{SIO})	viral shedding (m_i/m_r)
Type 1	↓ (weak protection)	↓	–
Type 2	↓↓ (strong protection)	↓↓	↑

Fig. 10 compares the weak and strong vaccines when the vaccine-modified susceptibility (m_s) is lower than the threshold value m_s^* (Eq. (8)). We see here that the average attack rate (A) and the final size (F) decrease as the vaccine coverage increases for both vaccine types. However, A_v and A_n increase for the Type 2 vaccine (bottom left panel). We also see that F_v will increase for both types of vaccine. There is some evidence to show that influenza vaccination can reduce the rate at which severe infection outcomes can occur in vaccinated individuals, compared to non-vaccinated individuals (CDC, 2020c). That is, the relative risk of a severe infection outcome

$$\mathrm{RR_{SIO}} = m_{\mathrm{SIO}} \frac{A_v}{A_n}, \tag{16}$$

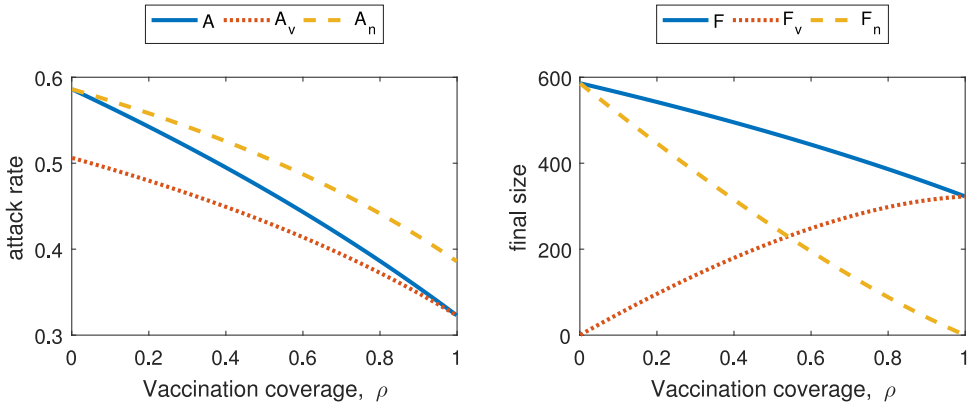

(a) Type 1 vaccine, $m_i/m_r = 1$, $m_s = 0.8$.

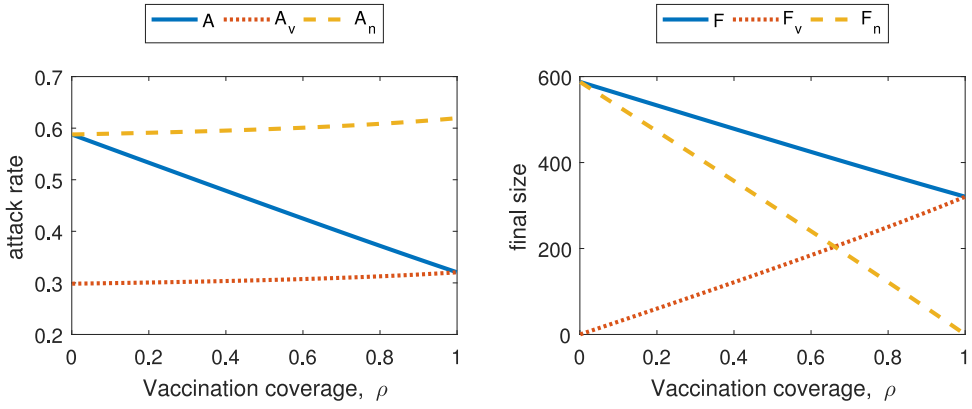

(b) Type 2 vaccine, $m_i/m_r = 2$, $m_s = 0.4$.

Fig. 10. Attack rate and epidemic final size for the comparison between a weak and strong vaccine. The attack rates A, A_v, and A_n (left column) and epidemic final sizes F, F_v and F_n (right column) are shown for two different hypothetical vaccines shown in Table 2. Right (left) panels represent the total number of infecteds (attack rate) for the general population (solid curve), and the vaccinated (dotted curve) and non-vaccinated (dashed curve) individuals. For Type 1 [Type 2] vaccine, we put $m_s = 0.8$ [$m_s = 0.4$] and $m_i/m_r = 1$ [$m_i/m_r = 2$], yielding $m_s^* = 1$ [$m_s^* = 1/2$]. In both cases, $m_s < m_s^*$, $R_0 = 1.5$, $\gamma = 0.33$, $\delta = 0$ and all other parameters are given in Table 1.

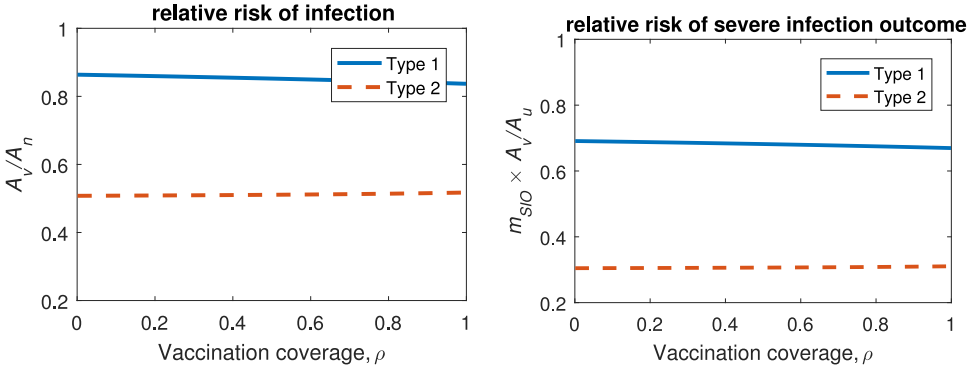

Fig. 11. Relative risk of infection and severe infection outcome for vaccinated individuals for a weak and strong vaccine. The left and right panels show the relative risks of infection (A_v/A_n) and severe infection outcome ($m_{SIO} \times A_v/A_n$) of vaccinated individuals, respectively. Solid (dashed) lines denote the weak (strong) vaccine. Here, the weak protection effect assumes $m_s = 0.8$, m_{SIO}=0.8 and $m_i/m_r = 1$ and the strong vaccine assumes $m_s = 0.4$, m_{SIO}=0.6 and $m_i/m_r = 2$. Also, $R_0 = 1.5$, $\gamma = 0.33$ days^{-1}, $\delta = 0$. Here, $m_s^* = 0.5$‘ and $m_s < m_s^*$.

with $0 < m_{SIO} < 1$, is reduced. Fig. 11 compares the relative risk of infection and relative risk of severe infection outcome for vaccinated individuals depending on the type of vaccine. Note that the relative risks of infection and severe infection outcome for vaccinated individuals is below unity for both types of vaccine, indicating that vaccination will reduce the infection and severe infection outcome risks of these individuals. We also note that, as expected, the Type 2 vaccine has a lower relative risk of infection, and that, since m_{SIO} is smaller for Type 2 vaccines, relative risk of severe infection outcome is lower when the population is vaccinated with Type 2 vaccines. Finally, we also see that, since $0 < m_{SIO} < 1$ the relative risk of severe infection outcome is smaller than the relative risk of infection, and that, since m_{SIO} is smaller for the Type 2 vaccine, the percent decrease between the Type 1 and Type 2 vaccines in the relative risk of severe infection outcome is greater than the percent decrease in the relative risk of infection.

4. Discussion

It is commonly acknowledged that vaccination against seasonal influenza decreases susceptibility and decreases infectivity in vaccinated individuals. A recent finding (Yan et al., 2018) shows an association between vaccination and increased viral shedding of seasonal influenza, suggesting that there may be an increase in infectivity in vaccinated individuals. Although the positive correlation between vaccination history and the increased viral shedding shown in Yan et al. (2018) is based on the small number of samples and the result is not yet verified by other studies, it is reasonable to assume that the viral shedding curve of an infected individual over the course of infection can be changed by the prior immunization (Belshe et al., 2000; Cao et al., 2015; Deiss et al., 2015; Talbot et al., 2005; VanWormer et al., 2014; Yan et al., 2018). Here, we assessed the effectiveness of an influenza vaccination program (i.e., R_v, attack rate, final size, CFR, death rate) considering changes in vaccine-modified susceptibility m_s and vaccine-modified viral shedding m_i/m_r. We found that with an increase in pathogen shedding from vaccinated yet infected individuals, the total attack rate may be reduced, even when the attack rates for both the vaccinated and non-vaccinated subpopulations are increased. By studying a relation between the vaccine-modified effects at the epidemic threshold, we observed that a higher vaccination coverage with a lower basic reproduction number allows less strict vaccine-modified susceptibility and viral shedding. When vaccinated individuals are less susceptible than non-vaccinated individuals, the attack rate of the vaccinated individuals is less than the attack rate of non-vaccinated individuals regardless of vaccine coverage or other vaccine-modified effects. In comparison, the final size of vaccinated individuals can exceed the final size of non-vaccinated individuals with high vaccine coverage even in the case when vaccinated individuals are less susceptible than non-vaccinated individuals. Vaccinating a population by a vaccine with strong protection effects would result in lower relative risk of infection and severe infection outcomes for vaccinees as well as the total number of influenza deaths, however, this may increase the CFR. Finally, vaccinating the population by a vaccine with strong protection effect would result in a lower relative risk of infection and complications for vaccinated individuals.

Acknowledgements

The authors thank Dr. Safia Athar for her help in document formatting. The work has been supported in part by the Natural Science and Engineering Research Council of Canada. (both the Discovery Grant (JMH, JW) and the Industrial Research Chair Program (Grant number:105588-2011 (JW))), the Canada Research Chair Program (grant number: 230720 (JW)) and the York Research Chair Program (JMH). JW has also been funded by the Fields-CQAM Interdisciplinary Program.

References

Arino, J., Brauer, F., Van Den Driessche, P., Watmough, J., Wu, J., 2007. A final size relation for epidemic models. Math. Biosci. Eng. 4 (2), 159.

Basta, N.E., Halloran, M.E., Matrajt, L., Longini, I.M., 2008. Estimating influenza vaccine efficacy from challenge and community-based study data. Am. J. Epidemiol. 168 (12), 1343–1352.

Belshe, R.B., Gruber, W.C., Mendelman, P.M., Mehta, H.B., Mahmood, K., Reisinger, K., Treanor, J., Zangwill, K., Hayden, F.G., Bernstein, D.I., Kotloff, K., 2000. Correlates of immune protection induced by live, attenuated, cold-adapted, trivalent, intranasal influenza virus vaccine. J. Infect. Dis. 181 (3), 1133–1137.

Biggerstaff, M., Cauchemez, S., Reed, C., Gambhir, M., Finelli, L., 2014. Estimates of the reproduction number for seasonal, pandemic, and zoonotic influenza: a systematic review of the literature. BMC Infect. Dis. 14 (1), 480.

Cade, B.S., Noon, B.R., 2003. A gentle introduction to quantile regression for ecologists. Front. Ecol. Environ. 1 (8), 412–420.

Cao, P., Wang, Z., Yan, A.W., McVernon, J., Xu, J., Heffernan, J.M., Kedzierska, K., McCaw, J.M., 2016. On the role of CD8+ T cells in determining recovery time from influenza virus infection. Front. Immunol. 7, 611.

Cao, P., Yan, A.W., Heffernan, J.M., Petrie, S., Moss, R.G., Carolan, L.A., Guarnaccia, T.A., Kelso, A., Barr, I.G., McVernon, J., Laurie, K.L., 2015. Innate immunity and the inter-exposure interval determine the dynamics of secondary influenza virus infection and explain observed viral hierarchies. PLOS Comput. Biol. 11 (8), e1004334.

Carrat, F., Vergu, E., Ferguson, N.M., Lemaitre, M., Cauchemez, S., Leach, S., Valleron, A.J., 2008. Time lines of infection and disease in human influenza: a review of volunteer challenge studies. Am. J. Epidemiol. 167 (7), 775–785.

CDC, Clinical signs and symptoms of influenza, Feb 17, 2020a. https://www.cdc.gov/flu/professionals/acip/clinical.htm.

CDC, How flu spreads, Feb 17, 2020b. https://www.cdc.gov/flu/about/disease/spread.htm.

CDC, Study shows flu vaccine reduces risk of severe illness, Feb 17, 2020c. https://www.cdc.gov/flu/spotlights/vaccine-reduces-risk-severe-illness.htm.

Deiss, R.G., Arnold, J.C., Chen, W.J., Echols, S., Fairchok, M.P., Schofield, C., Danaher, P.J., McDonough, E., Ridor, M., Mor, D., Burgess, T.H., 2015. Vaccine-associated reduction in symptom severity among patients with influenza A/H3N2 disease. Vaccine 33 (51), 7160–7167.

Earn, D.J., Andrews, P.W., Bolker, B.M., 2014. Population-level effects of suppressing fever. Proc. R. Soc. B. 281 (1778), 20132570.

Fiore, A.E., Uyeki, T.M., Broder, K., Finelli, L., Euler, G.L., Singleton, J.A., Iskander, J.K., Wortley, P.M., Shay, D.K., Bresee, J.S., Cox, N.J., 2010. Prevention and control of influenza with vaccines: recommendations of the Advisory Committee on Immunization Practices (ACIP). MMWR Recomm. Rep. (59) 1–62.

Fireman, B., Lee, J., Lewis, N., Bembom, O., Van Der Laan, M., Baxter, R., 2009. Influenza vaccination and mortality: differentiating vaccine effects from bias. Am. J. Epidemiol. 170 (5), 650–656.

Jackson, L.A., Gaglani, M.J., Keyserling, H.L., Balser, J., Bouveret, N., Fries, L., Treanor, J.J., 2010. Safety, efficacy, and immunogenicity of an inactivated influenza vaccine in healthy adults: a randomized, placebo-controlled trial over two influenza seasons. BMC Infect. Dis. 10 (1), 71.

Osterholm, M.T., Kelley, N.S., Sommer, A., Belongia, E.A., 2012. Efficacy and effectiveness of influenza vaccines: a systematic review and meta-analysis. Lancet Infect. Dis. 12 (1), 36–44.

Porta, M., 2014. A Dictionary of Epidemiology, sixth ed. Oxford University Press.

Talbot, T.R., Crocker, D.D., Peters, J., Doersam, J.K., Ikizler, M.R., Sannella, E., Wright, P.F., Edwards, K.M., 2005. Duration of virus shedding after trivalent intranasal live attenuated influenza vaccination in adults. Infect. Control Hosp. Epidemiol. 26 (5), 494–500.

Van den Driessche, P., Watmough, J., 2008. Further notes on the basic reproduction number. In: Brauer, F., van den, D.P., Wu, J. (Eds.), Mathematical Epidemiology. Lecture Notes in Mathematics, Vol. 1945. Springer, Berlin, Heidelberg, pp. 159–178.

VanWormer, J.J., Sundaram, M.E., Meece, J.K., Belongia, E.A., 2014. A cross-sectional analysis of symptom severity in adults with influenza and other acute respiratory illness in the outpatient setting. BMC Infect. Dis. 14 (1), 231.

Wong, J.Y., Kelly, H., Ip, D.K., Wu, J.T., Leung, G.M., Cowling, B.J., 2013. Case fatality risk of influenza a (H1N1pdm09): a systematic review. Epidemiology 24 (6).

Yan, A.W., Cao, P., Heffernan, J.M., McVernon, J., Quinn, K.M., La Gruta, N.L., Laurie, K.L., McCaw, J.M., 2017. Modelling cross-reactivity and memory in the cellular adaptive immune response to influenza infection in the host. J. Theor. Biol. 413, 34–49.

Yan, J., Grantham, M., Pantelic, J., de Mesquita, P.J., Albert, B., Liu, F., Ehrman, S., Milton, D.K., 2018. EMIT consortium. Infectious virus in exhaled breath of symptomatic seasonal influenza cases from a college community. PNAS 115 (5), 1081–1086.